International Journal of GEOMATE, Sept., 2021, Vol.21, Issue 85, pp.71-83
ISSN: 2186-2982 (P), 2186-2990 (O), Japan, DOI: https://doi.org/10.21660/2021.85.j2217
Geotechnique, Construction Materials and Environment

SEISMIC PROPERTIES AND FRACTAL DIMENSION OF SUBDUCTION ZONE IN JAVA AND ITS VICINITY USING DATA FROM 1906 TO 2020

*Yunalia Muntafi[1,2] and Nobuoto Nojima[3]

[1] Graduate School of Engineering, Gifu University, Japan; [2] Faculty of Civil Engineering and Planning, Universitas Islam Indonesia, Indonesia; [3] Faculty of Engineering, Gifu University, Japan

*Corresponding Author, Received: 28 May 2021, Revised: 13 July 2021, Accepted: 26 July 2021

ABSTRACT: As the highest population density area in Indonesia which experienced tsunami-earthquakes in 1921 (Mw7.6), 1994 (Mw7.6), and 2006 (Mw7.7), the Java region has the threat of seismic activities, which could inflict great losses. Several seismic hazard studies have been carried out, but essential parameters have not been explicitly identified, and data on earthquake return periods remain limited. This study addresses such issues by identifying the seismic properties, including the seismic activity (a-value), frequency magnitude distribution related to the tectonic parameter (b-value), fractal dimension (D), and maximum magnitude (Mmax) of the subduction zone along the Java Island. The earthquake data used are those from 1906 to 2020. The research started with the processing of earthquake data, continued by determining the a-b values of Gutenberg-Richter relation using the maximum likelihood method. The fractal dimensions were estimated based on the fracture distance and the maximum magnitudes were calculated using some return period scenarios. Our results show that low seismic activity levels are relatively consistent with a low b-value pattern. The lowest b-values are in the south coast of West Java and the south coast of Central-East Java. Based on the fractal dimension analysis, the interplate zones have a more complex fault geometry than intraplate ones. The maximum earthquake magnitude estimation of each subduction segment is presented and discussed comprehensively in this paper. These findings will redound to the benefit of earthquake and tsunami disaster mitigation and earthquake modeling efforts for future seismic hazard studies.

Keywords: Earthquake, Java subduction, Gutenberg-Richter Law, fractal dimension, maximum magnitude

1. INTRODUCTION

Geographically, Java Island is located in the subduction zone (collision) between the Indo-Australian and Eurasian tectonic plates. The Indo-Australian plate moves northward and sinks under the Eurasian tectonic plate, forming a subduction zone in the south of Java Island. The plate motion speed in the western region of northern and central Sumatra ranges from 52 to 57 mm/yr and the movement in the western region of South Sumatra is around 60 mm/yr. Meanwhile, the speed of plate movement in the south of Java is around 80 mm/yr [1]. At the Central Java trench, the subduction zone strike is relatively perpendicular with the plate motion direction [2]. The length of Sunda trench along Sumatra and Java Island, the high rate of plate convergence, and the high deficit rate in several areas in the south of Java that trigger energy accumulation underlie many scientists to argue that potentially powerful earthquake and tsunami would affect this region. Becoming one of the world's most densely populated areas, Java Island and its surroundings face a threat of seismic activities which can cause significant losses. The large earthquakes with magnitude greater than Mw 7.0, including tsunami-earthquakes in 1921 (Mw 7.6), 1994 (Mw 7.6), 2006 (Mw 7.7), and 2009 (Mw 7.3) that have occurred along the Java subduction are presented in Table 1.

Table 1 Earthquake in Java with magnitude of Mw > 7.0 and its impact [3-7]

Year	Magnitude (Mw)	Impact				Tsunami (height)
		killed	missing	injured	building damage	
2009	7.3	111	27	1,297	25,000	1 m
2006	7.7	637	164	9,245	1,623	5-8 m
1994	7.6	429	30	723	2,025	13.9 m
1943	7.1	213	-	2,096	2,800	-
1926	7.1	NA	NA	NA	NA	-
1921	7.6	NA	NA	NA	NA	10 cm

NA: Not Available

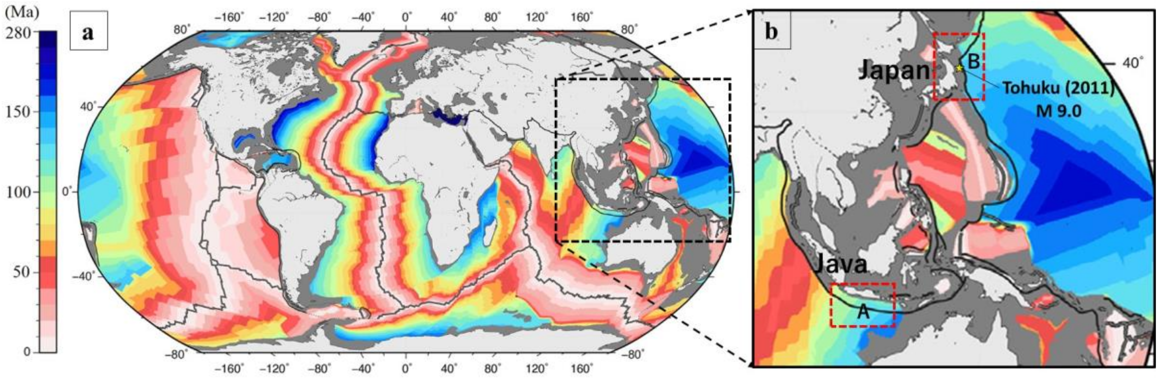

Fig.1 The oceanic crustal age [8,9]. (a) Seafloor age global map generated using the Generic Mapping Tools; (b) Seafloor age in south of Java and east-north side of Japan (zoomed-in)

Learning from the major earthquake experienced by Japan in 2011, the seafloor of eastern Japan (B area) which is slightly older than that of southern Java (A area) shown in Fig.1 [8] was able to produce an earthquake with magnitude of M9.0 on March 11, 2011, in the Tohuku region. The surface energy of the earthquake was two times higher than the energy of the 2004 tsunami in Aceh, Indonesia, which reached $1.9 \pm 0.5 \times 10^{17}$J [10]. The terrible tsunami attacking Tohuku reached a height of more than 39 m and left more than 24 thousand people missing or dead [11].

Several studies related to tsunami wave modeling with the certain earthquake scenarios for the south Java coastal area have been created. Hartoko et al. [12] generated spatial tsunami wave modeling with earthquake scenarios of M8.4, M7.9, and M7.0 for the south of West Java (Serang), south of Central Java (Bantul), and south of East Java (Banyuwangi), respectively. Based on the model constructed for the three coastal areas in south of Java, two tsunami waves can reach a height of 2 to 8 m with an interval of about 30 minutes. In addition, the result also stated that a 2-m wave will hit the coastal area after 60 minutes of travel time. Meanwhile, Widiyantoro et al. [13] modeled tsunami waves using the worst-case scenario of subduction earthquakes, in which two segments of megathrust along the Java region simultaneously rupture. The results show that the earthquake scenario can trigger ~ 20 m and ~ 12 m tsunami waves on the south coast of West and East Java, respectively. In the previous studies, the essential seismic parameters have not been explicitly identified, and data on earthquake return periods remain limited. This study addresses such gaps by identifying the seismic properties, including the seismic activity (a-value), size distribution (b-value), fractal dimension (D), and maximum magnitude (Mmax) of the subduction zone along the Java Island as an effort to conduct earthquake and tsunami disaster mitigation.

2. RESEARCH SIGNIFICANCE

The findings of this study will contribute to the earthquake-tsunami disaster mitigation and earthquake modeling efforts for future seismic hazard studies. Seismic activity rate and frequency-magnitude distribution investigated related to the tectonic condition (a-value and b-value) can be used as the main parameters for conducting the seismic hazard analysis. In addition, the estimated maximum magnitude (Mmax) of each segment can be used as a reference for the tsunami and seismic hazard probabilistic modeling influenced by the subduction earthquake sources in Java and its vicinity. This study also presented the seismic gaps areas and fault geometry complexity that can be considered in the earthquake and tsunami disaster mitigation plan.

3. METHODS

3.1 Earthquake Data and Processing

The earthquake data were compiled from the Agency of Meteorology, Climatology, and Geophysics (BMKG) Indonesia with relocated hypocenter data using TeletomoDD method [14]. In addition, earthquake data from the International Seismological Center (ISC) [15] for historical earthquakes occurring in and around Java Island were also collected, including the EHB (Engdahl, van der Hilst, and Buland) improved earthquake data set [16]. From these data sources, a catalog of earthquakes from 1906 to September 2020 with magnitude of Mw $\geq$ 4.5 was obtained. The earthquake data were then converted into moment magnitude (Mw) scale. For this purpose, we collected all available earthquake dataset of the Indonesia region (1906 to September 2020) to get the correlation of body-wave magnitude (mb) and surface-wave magnitude (Ms) into Mw. The mb-Mw dataset (21,853 events) and Ms-Mw dataset (13,402 events) compiled were then plotted into the graphs, which are presented in Fig.2.

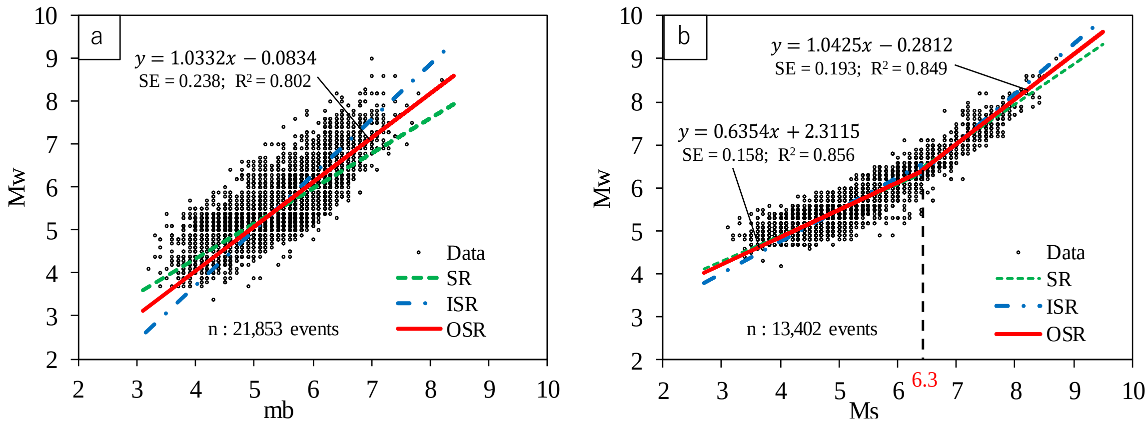

Fig.2 Magnitude scale relationships of Indonesia earthquake events dataset. (a) mb-Mw ; (b) Ms-Mw

The conversion for body-wave magnitude (mb) and surface-wave magnitude (Ms) of all earthquake events in the Indonesian region were determined based on three regression models, namely Standard Regression (SR), Inverted Standard Regression (ISR), and Orthogonal Standard Regression (OSR). The accuracy tests for magnitude correlation were performed including the R^2 test and standard error (SE) test. The OSR shows the best-fit relationship for the magnitude correlation for mb-Mw and Ms-Mw to be used in this study. The magnitude conversion formula is as follows:

$$M_w = 1.0332 m_b - 0.0834 \quad (1)$$

for the magnitude range of 3.2 $\leq$ mb $\leq$ 8.2; SE = 0.238 and R^2 = 0.802

$$M_w = 0.6354 M_s + 2.3115 \quad (2)$$

for the magnitude range of 3.1 $\leq M_s \leq$ 6.3; SE = 0.158 and R^2 = 0.856

$$M_w = 1.0425 M_s - 0.2812 \quad (3)$$

for the magnitude range of 6.4 $\leq M_s \leq$ 8.7; SE = 0.193 and R^2 = 0.849

A number of declustering algorithms were developed based on different assumptions and recorded data. Five of the most well-known declustering algorithms are provided in [17-21]. In 2019, Teng and Baker [22] evaluated several declustering algorithm models for earthquake data and applied it to a seismic hazard analysis in two cities in the USA. The results show that the Gardner and Knopoff and Zhuang methods using the epidemic type of aftershock sequence (ETAS) [23,24] potentially result in a negligible likelihood of massive earthquakes being mainshocks and overestimate the effects of foreshock. Their observations shed light on both Reasenberg and Zaliapin and Ben-Zion declustering algorithms provide better results for a seismic hazard analysis. In this study, we applied the Reasenberg method for declustering the earthquake data which was also carried out by [25] for an earthquake analysis in East Java, Indonesia.

3.2 The FMD and a-b Parameter

The a and b parameters, commonly known as a-values and b-values are used to determine the seismic activity and frequency-magnitude distribution (FMD) in correlation with the tectonic conditions of the study area, which become an essential parameter in the seismic hazard analysis. In this study, we followed the FMD provided by Gutenberg and Richter [26] that has been verified for global and regional seismicity. The equation is:

$$\log(N) = a - bM \quad \text{or} \quad N = e^{\alpha - \beta M} \quad (4)$$

where N describes the cumulative number of earthquakes with magnitude equal to or greater than M, a and b are constants, indicating the seismicity activity and the log-linear relation’s slope, respectively, and e is a natural number. We used the Maximum Likelihood Method (MLM) as the most widely accepted method to calculate the b-value given by Utsu [27]:

$$b = \frac{1}{\bar{M} - M_o} \log_{10} e \quad (5)$$

The a-value was estimated using the formula of Wekner, 1965 in [28] as follows:

$$a = \log N(M \geq M_o) + \log(b \ln 10) + M_o b \quad (6)$$

where $\bar{M}$ denotes the average magnitude and M_o is the minimum magnitude of earthquake data, in which we used the magnitude completeness, Mc parameter.

3.3 Fractal dimension and maximum magnitude

The fractal dimension (D) in a seismicity study can be determined based on the relationship of the linear regression slope between the logarithm of the fracture distance (r_n) from the earthquake source and the logarithm of the integral correlation constant C(r) [29]. We calculated the D using that correlation which was also used in [5] and [30] as follows:

$$D = \lim_{r \to 0} \frac{Log\ C(r)}{\log r_n} \tag{7}$$

C(r) is estimated based on a set of points of clustering using the following relation:

$$\mathrm{C(r)} = \frac{2}{N(N-1)} N(R < r) \tag{8}$$

N(R<r) represents the number of event pairs separated by a distance R in a cluster with a distance smaller than r.

Earthquakes occur because of the accumulation of pressure, and the process of releasing energy is related to time. Consequently, to conduct the seismic hazard analysis, the estimation of maximum earthquake magnitude must be considered. The maximum magnitude (Mmax) for each segment was calculated using the following magnitude equation of Hanks and Kanamori [31] and Wells and Coppersmith [32]:

$$\mathrm{M} = \tfrac{2}{3} \log M_o - 10.7 \tag{9}$$

$$\mathrm{M} = 4.07 + 0.98 \log A \tag{10}$$

where A is the area of each segment, and the seismic moment, M_o represents the meaningful physical relationship between the size of earthquake and rupture parameters which is defined as:

$$M_o = \mu \bar{D} A \tag{11}$$

where μ is the shear modulus (3 x 10^{11} dyne/cm^2) assumed to be the same for all segments, and $\bar{D}$ is the average displacement determined from the slip rate ($\dot{D}$) and return period (Tr), so then the formula becomes:

$$\mathrm{M} = \tfrac{2}{3} \log\ (\mu\ \dot{D}\ Tr\ A) - 10.7 \tag{12}$$

4. RESULTS AND DISCUSSION

The earthquake data from the sources mentioned in the methods section consist of 8269 events and were converted into a magnitude moment scale (Mw) using Eq. (1-3). In this study, the declustering process employed the Reasenberg method using Zmap software [33]. The declustering removed 1226 earthquake events, resulting in a total of 7043 events. This new compiled catalog is then plotted in Fig.3 based on the depth and magnitude of each earthquake event.

The earthquakes distribute along plate junctions had decreased within the year of 2011-2016 but risen again after 2017, even until 2020 the trend remained significantly upward up to magnitude of 7.0. Meanwhile, earthquake data obtained before 1965 were large earthquakes with a magnitude of Mw > 5.5. This was because of the limited instrument capability to record the earthquake data with a smaller magnitude. Even before 1950, the recorded earthquakes were those with a magnitude greater than Mw 6.0.

Likewise, the history of the earthquakes with a depth of > 100 km can only be recorded after 1960. Based on these earthquake distribution data, it can be said that the recording of earthquake events is getting better after 1965. It can also be seen from the figure that shallow earthquakes dominated with a depth of $\leq$100 km. However, there are only a few earthquakes that occur at a depth of 300-500km. Besides, several earthquakes recorded up to a depth of 600 km.

The earthquake event plot presented in Fig.3 also reveals the two densely inhabited earthquake epicenter locations (A and B area). In the A area, there was an experience of major earthquake in 2006 with a magnitude of Mw 7.7, while in the B area, an earthquake occurred in 1994 (Mw 7.6), both of which were followed by a tsunami. On the contrary, there are seismic gap areas in the south coast of Java and its adjacent regions, which are indicated by yellow shaded areas (I, II, and III) extending about 385km, 350km, and 270km long, respectively.

In the seismic gap zone II, there is a large earthquake occurred in 1921 (Mw 7.6). The earthquake in 1921 was in the outer-rise zone, which was also followed by a tsunami recorded at Cilacap. Some earthquakes occurred in the immediate vicinity of the Java trench or commonly known as outer-rise earthquakes. Almost all the outer-rise earthquakes took place along the uppermost part of the subduction interface are shallow earthquakes with a depth of not more than 50km; only a few of them are up to 100km.

Seismic gap zones I and III, which are 385km and 270km long are also essential to be considered, especially in the modeling of earthquake and tsunami analysis. The existence of these seismic gaps indicates the accumulation of earthquake energy, thus providing the possibility of large earthquakes in the future. Some simulations using the worst-case scenarios will be beneficial for disaster mitigation efforts.

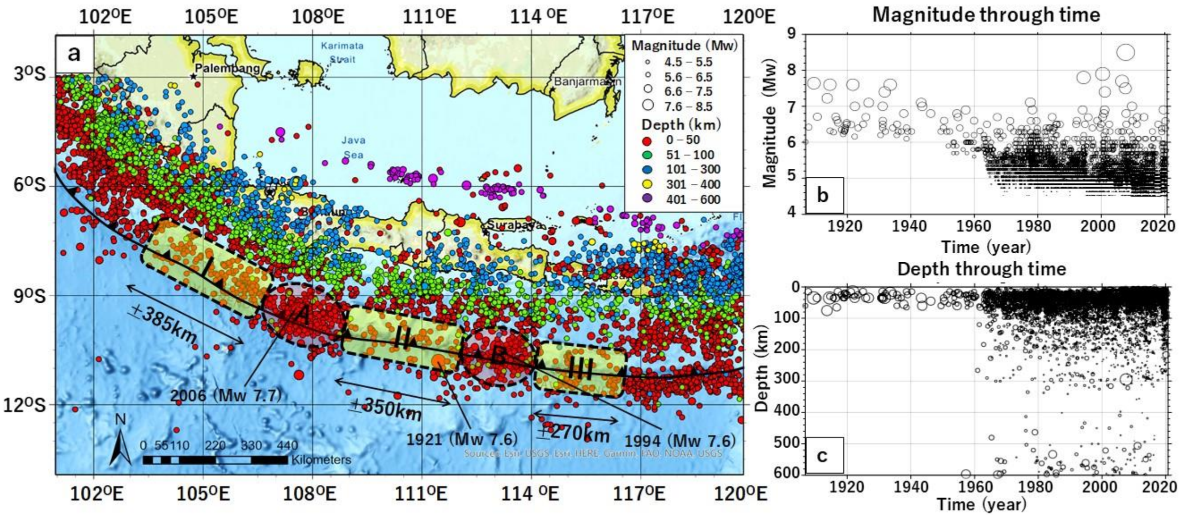

Fig.3 Earthquake catalog of Java island and adjacent region period 1906 to September 2020 with magnitude Mw≥4.5. (a) Epicenter distribution; (b) Earthquake depth by time; (c) Earthquake magnitude by time

In order to obtain more detailed information about the mechanism and characteristics of the Indo-Australian plate subduction, which forces the Eurasian plate and affects the geological conditions of Java Island, we carried out a seismicity cross-section. A total of 18 cross-sections (CS) were created along the Java trench and adjacent regions based on the epicenter data mapped to a depth of 600km. Each cross-section describes the distribution of earthquake events, subduction dip angle, and earthquake depth per segment, which is presented in Fig.4.

Based on the cross-section results (Fig.4), it is found that the subduction dip angle on the southern side of South Sumatra (CS 1-4) is more gentle than the southern subduction angle in Java Island, which is around 12-13^{o} for the interplate zone and 40-42^{o} for the intraplate zone. It can also be seen in CS 1-4 that the earthquakes occurring in the southern part of Sumatra are less than 300 km deep. Meanwhile, the subduction angle under the island of Java ranges from 13^{o} to 14^{o} for the interplate zone and from 43^{o} to 47^{o} for the intraplate zone. It can also be seen from CS 5-14 that the earthquakes in Java reached a depth of up to about 600 km. Deep earthquakes began to occur at the location of the Sunda strait to the east. This is related to the age of the submerged crust under southern Sumatra, which is younger than Java (Fig.1). In addition, the seafloor age is correspondingly older to the east, leading to a larger dipping angle of subduction. This result ties well with previous studies wherein the oceanic crust under Java is heavier, making it sinks more easily [34], indicating that the dip angle of subduction in this area is larger than that in the Sumatra trench.

For Bali and Sumbawa regions, the dip angle of the subduction zone is relatively smaller than Java but greater than the southern side of South Sumatra, which is 42-44^{o} (CS 15-18). Moreover, the depth of earthquakes reached up to 600km. The earthquakes with a depth of up to 600 km are in the northern regions of Central Java, East Java, and Bali-Sumbawa.

In investigating the seismic activity rate and frequency-magnitude distribution of Gutenberg-Richter relation, we conducted the calculation of a-values and b-values in detail using grid cell of 0.1^{o}x 0.1^{o} using Eq. (4), (5), and (6). These a-values and b-values were calculated based on the earthquake data from the earthquake catalog between 1906 and September 2020. This study used Zmap software to compute the spatial variation of a-value and b-value for the study area with a constant radius of 100km. The spatial variation of a-value and b-value are displayed in Fig.5.

The picture reveals a similar pattern of a-value and b-value along the Java trench and the surrounding area. The region with a low a-value corresponds to a low b-value region. The spatial variation of a-value ranges from 5 to 12, while the b-values range from 0.7 to 1.8. In general, the a-values and b-values in the southern part of Sumatra are dominated by dark blue color, indicating low a-values and b-values. In the western part of Java, the b-value is around 0.8 to 1.3. There are several points with b-value of up to 1.5 in the north-west of Java, which is correspondingly smaller to the center region and larger to the southern part of Bali-Sumbawa. The yellow stars marking the large earthquakes of Mw > 6.5 are predominantly located in relatively low a- and b-value regions. The lower b-value indicates the higher stress in an earthquake source zone.

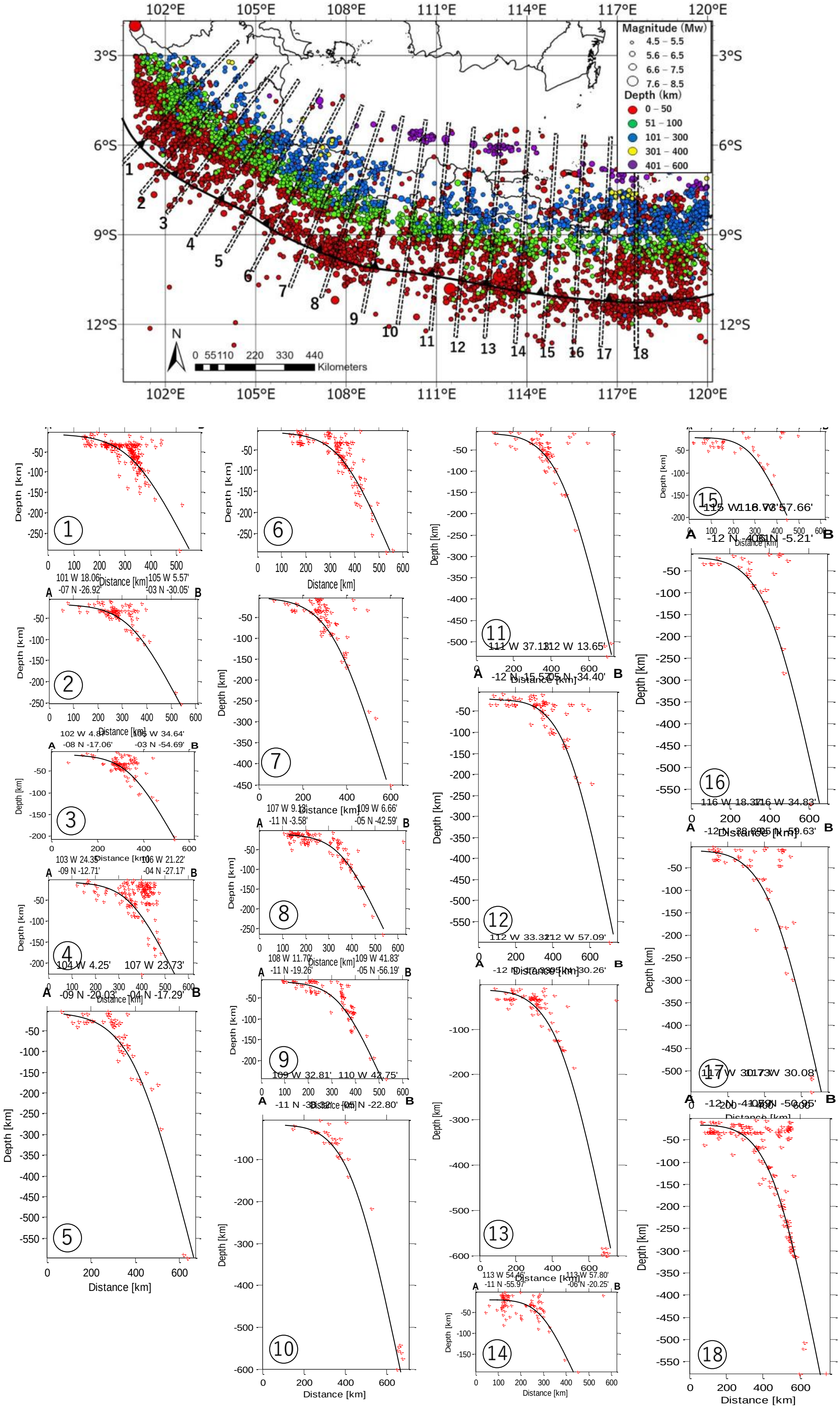

Fig.4 Cross-section of earthquake distribution along Java and its vicinity

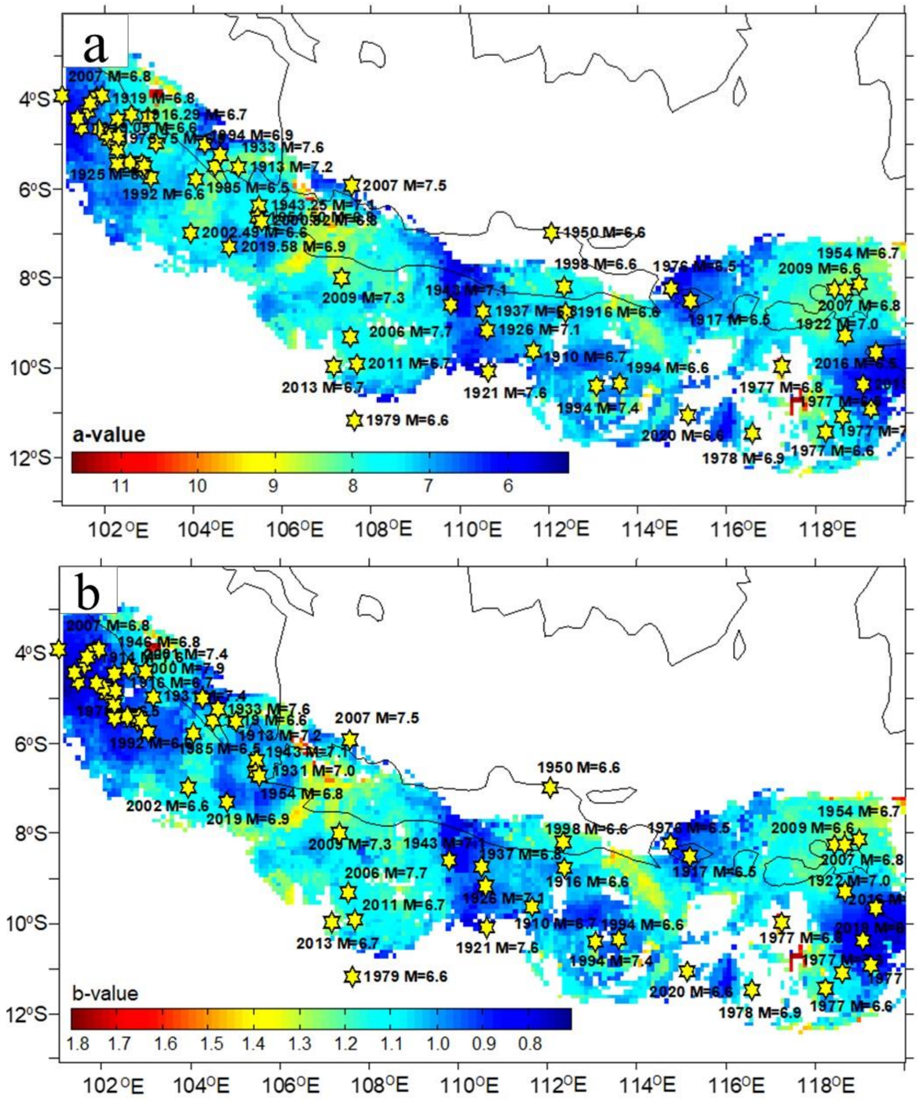

Fig.5 Spatial a-value and b-value variation of Java and adjacent region. (a) a-value (b) b-value

To identify the seismicity of the subduction zone in more detail, we developed the segmentation model from previous research [35]. In the previous research, the subduction zone considered was only in the southern part of southern Sumatra to the south of Central Java and parts of East Java because the research area was taken up to a radius of 500 km from the Special Capital Region of Jakarta. In this study, the subduction zone along the Java trench and adjacent regions was considered. We modeled six segments for each interplate and intraplate zone: eight segments for Java subduction, two segments for the subduction in the south of southern Sumatra, and two segments for Bali-Sumbawa. The FMD diagram for each segment is shown in Fig.6.

The figure shows the variation of cumulative and noncumulative frequency with earthquake magnitude for each subduction segment. The complete recording is indicated by magnitude completeness, Mc. Most of the segments have a value of Mc = 4.7, while the largest Mc value is in the IE-6 segment with Mc = 5.1. It is found in the figures that all the slopes in the FMD diagram are constant after the Mc value, indicating the level of completeness for the instrumental part of the compiled catalog. The slopes of segments IA-4 and IE-1 are relatively gentler, while IA-5, IE-3, and IE-6 have a steeper slope as shown in the FMD diagram. We can observe from the red line that the higher proportion of smaller magnitude events, the steeper the slope of FMD, indicating relatively few numbers of large magnitude events. These patterns follow the Gutenberg-Richter Law as in Eq. (4), which provides the a and b relationship. The a-value and b-value of each subduction segment were computed using Eq. (5) and (6). In this study, we also analyzed fractal dimensions using Eq. (7) and (8) to clarify the fault geometry of each segment. The results of a-b values and fractal dimensions are provided in Table2.

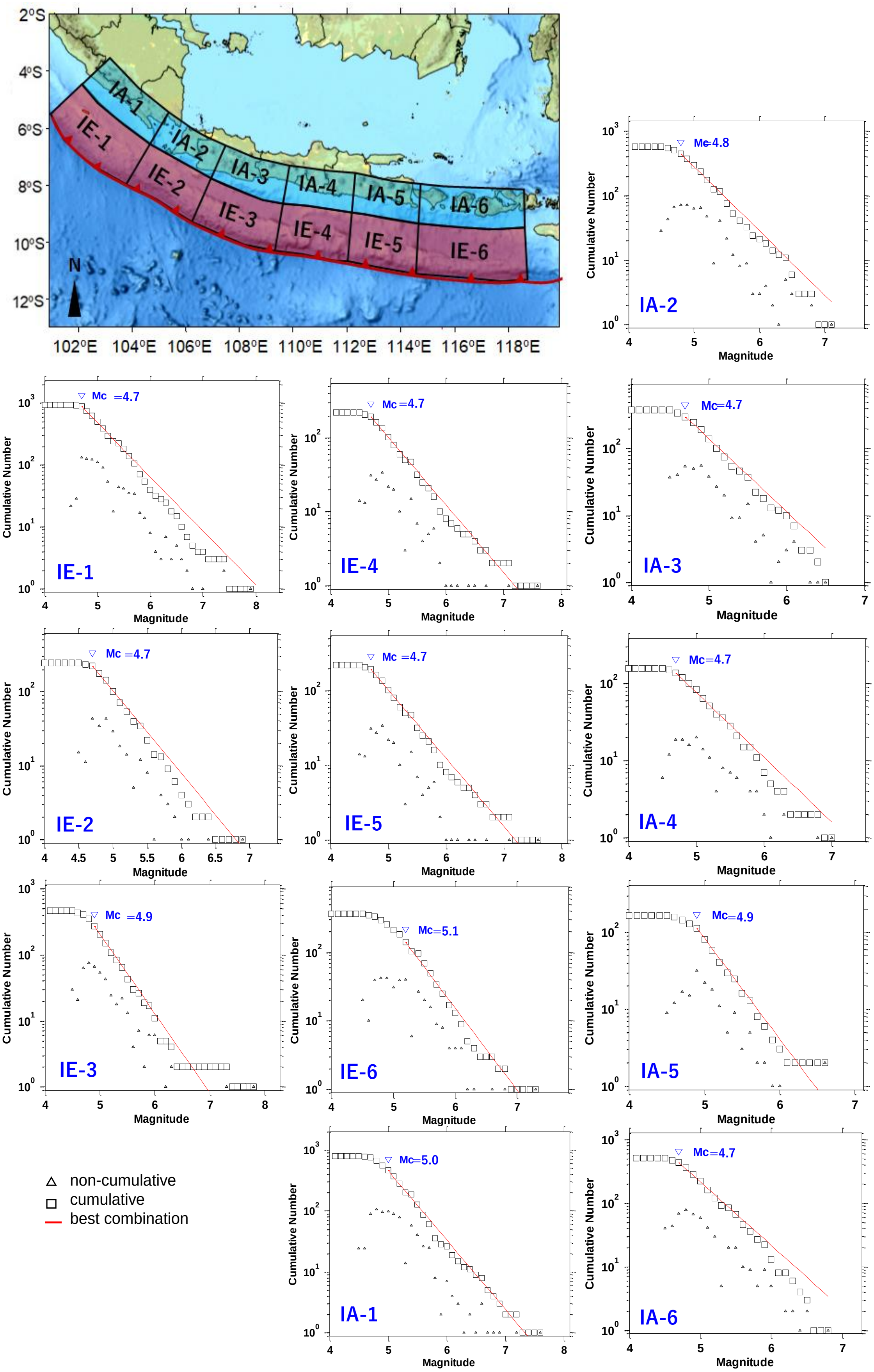

Fig.6 The frequency-magnitude distribution (FMD) of each subduction segment

Table 2 The a-b parameter and fractal dimension of each subduction segment

Subduction zone	Index	Segment	a	α	b	β	D
Interplate (IE)	IE-1	South Sumatra	4.99	11.49	0.87	2.01	2.32 ± 0.03
	IE-2	West Java	5.14	11.84	0.94	2.16	2.24 ± 0.03
	IE-3	West-Central Java	6.52	15.02	1.20	2.76	2.07 ± 0.02
	IE-4	Central-East Java	4.55	10.48	0.92	2.11	2.37 ± 0.02
	IE-5	East Java	5.57	12.83	1.06	2.44	2.13 ± 0.02
	IE-6	Bali-Sumbawa	6.61	15.22	1.20	2.76	2.05 ± 0.02
Intraplate (IA)	IA-1	South Sumatra	6.32	14.55	1.14	2.63	2.07 ± 0.02
	IA-2	West Java	5.46	12.57	0.99	2.29	2.25 ± 0.02
	IA-3	West-Central Java	5.81	13.38	1.09	2.51	1.96 ± 0.01
	IA-4	Central-East Java	4.18	9.63	0.84	1.94	2.27 ± 0.02
	IA-5	East Java	6.46	14.88	1.31	3.02	1.54 ± 0.01
	IA-6	Bali-Sumbawa	5.33	12.27	1.00	2.30	1.96 ± 0.03

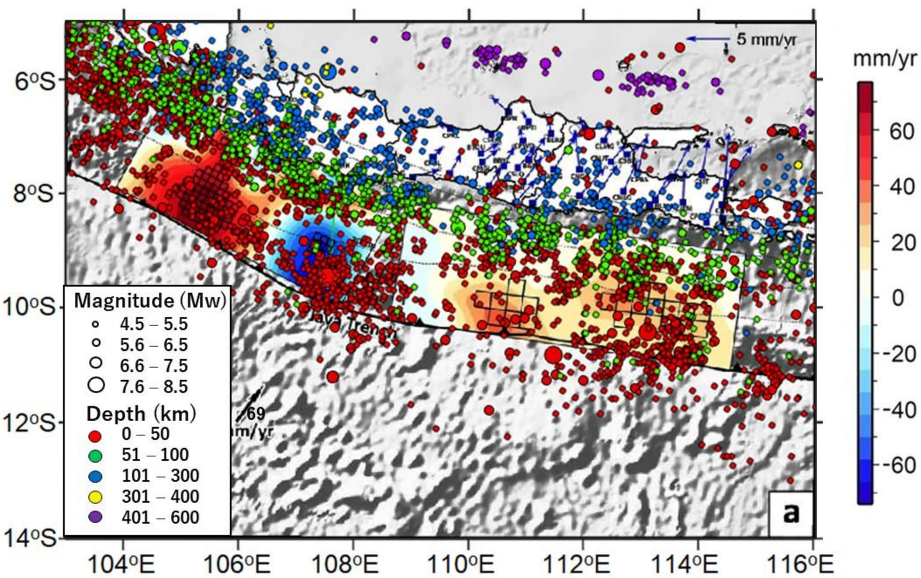

Fig.7 Slip deficit/excess rate along the Java Trench generated using GPS data with the epicenter distribution of this study. Left model provided in [10]; Right model created by [13]

The results clearly show that the a-values for twelve subduction segments vary from 4.18 to 6.61 and b-values are between 0.84 and 1.31. These findings are somewhat different from those of [36], which stated that the a-value and b-value for the subduction zone of Java Island are 7.39 and 1.28, respectively. However, these results are in agreement with the research conducted in the last 5 years by [37,38] although globally the b-value is ~ 1 for a seismically active region [39]. In more detail, the highest a-value and b-value of Java subduction interplate segment is in the IE-3 region, which has a steep slope of FMD diagram. It is evident that the steeper the slope, the higher b-value obtained. In contrast, the IE-2 region has a lower a-value and b-value, thus shedding light on the increasing potential for moderate to large earthquakes in this region.

This finding supports a previous study of slip deficit/excess along the Java trench [40] displayed in Fig.7 (left model) computed using continuous GPS data. The red areas of slip deficit correspond to the segment's location of a-value and b-value of this study that is associated with a low seismic activity and a high stress level in that tectonic zone.

Meanwhile, the IE-4 region has the lowest a and b value, while the IE-5 region has a slightly higher a and b value. Although the result for IE-4 region tends to be nearly correlated with the slip deficit map as in [13] (Fig.7, right model), the result for IE-5 region is somewhat different. Therefore, further research is required to determine the correlation between earthquake data and GPS data analysis during the same period.

The fractal dimension for six interplate segments obtained from D = 2.05 $\pm$ 0.02 to 2.37 $\pm$ 0.02, while those for intraplate segments are 1.54 $\pm$ 0.01 to 2.27 $\pm$ 0.02. The D values of interplate segments are relatively higher than those of the intraplate ones, indicating that the interplate zone has a more complex or irregular fault geometry. In general, the fractal dimensions and b-values of Java subduction segments show a negative correlation. The highest D value is in the Central-East Java segment (IE-4 and IA-4) which also has the lowest b-value. These values are relatively higher than the results from [1], but smaller than the results stated in [41].

In estimating the maximum earthquake magnitude, the Eq. (9) and (10) were applied using the return period from 100 years to 500 years with a calculation per 100 years for Eq. (11) and (12). The slip rate of the southern subduction segment of Java used is 4cm/yr [42]. The Mmax result is presented in Table 3 and the comparison is graphically displayed in Fig.8.

Table 3 The maximum magnitude (Mmax) estimation for interplate and intraplate segments

Subduction zone	Index	A (m^2)	Mw (Hanks and Kanamori, 1979) T=100yr	T=200yr	T=300yr	T=400yr	T=500yr	Mw (Wells and Coppersmith, 1994)
Interplate (IE)	IE-1	8.09.E+10	8.59	8.83	8.94	9.03	9.09	8.88
	IE-2	5.29.E+10	8.47	8.70	8.82	8.90	8.97	8.70
	IE-3	6.00.E+10	8.50	8.74	8.86	8.94	9.00	8.75
	IE-4	5.48.E+10	8.48	8.71	8.83	8.91	8.98	8.71
	IE-5	5.52.E+10	8.48	8.71	8.83	8.92	8.98	8.72
	IE-6	9.66.E+10	8.64	8.88	8.99	9.08	9.14	8.96
Intraplate (IA)	IA-1	5.92.E+10	8.50	8.74	8.85	8.94	9.00	8.75
	IA-2	4.02.E+10	8.39	8.62	8.74	8.82	8.89	8.58
	IA-3	4.29.E+10	8.40	8.64	8.76	8.84	8.91	8.61
	IA-4	4.28.E+10	8.40	8.64	8.76	8.84	8.91	8.61
	IA-5	4.36.E+10	8.41	8.65	8.76	8.85	8.91	8.62
	IA-6	7.65.E+10	8.57	8.81	8.93	9.01	9.07	8.86

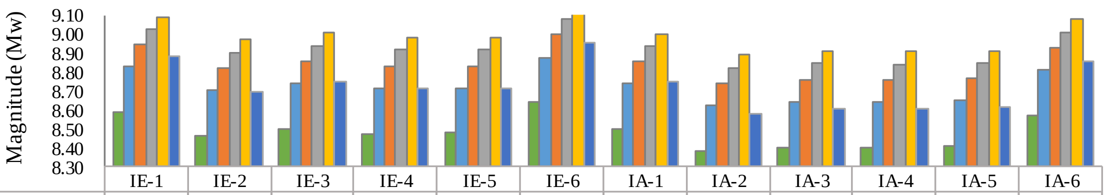

	IE-1	IE-2	IE-3	IE-4	IE-5	IE-6	IA-1	IA-2	IA-3	IA-4	IA-5	IA-6
HK-1979 (100yr)	8.59	8.47	8.50	8.48	8.48	8.64	8.50	8.39	8.40	8.40	8.41	8.57
HK-1979 (200yr)	8.83	8.70	8.74	8.71	8.71	8.88	8.74	8.62	8.64	8.64	8.65	8.81
HK-1979 (300yr)	8.94	8.82	8.86	8.83	8.83	8.99	8.85	8.74	8.76	8.76	8.76	8.93
HK-1979 (400yr)	9.03	8.90	8.94	8.91	8.92	9.08	8.94	8.82	8.84	8.84	8.85	9.01
HK-1979 (500yr)	9.09	8.97	9.00	8.98	8.98	9.14	9.00	8.89	8.91	8.91	8.91	9.07
WC-1994	8.88	8.70	8.75	8.71	8.72	8.96	8.75	8.58	8.61	8.61	8.62	8.86

Fig.8 The comparison between maximum magnitude of two methods. HK means Hanks and Kanamori method (1979); WC means Wells and Coppersmith method (1994)

Based on the calculation using some scenarios, the Java interplate segments have the potential to trigger earthquakes up to magnitude of Mw 8.47-9.00, while the Java intraplate can trigger an earthquake up to magnitude of Mw 8.39-8.91. The interplate segments in southern Sumatra and the southern part of Bali-Sumbawa have higher potential of earthquake magnitude than Java, which are up to Mw 8.59-9.09 and Mw 8.64-9.14, respectively. The results were calculated based on the assumption that all the tectonic energies in the Java trench were released seismically. For the Hanks and Kanamori method, apart from the segment area, the maximum magnitude is influenced by the return period; however, the Wells and Coppersmith formula is more influenced by dimension.

The results of estimated maximum earthquake magnitude using Wells and Coppersmith equation are between the result for a return period of 200 years and 300 years of Hanks and Kanamori method. Referring to the return period used in Indonesian Seismic Sources and Seismic Hazard Maps 2017 (Tr = 400 years) [42], the interplate segment in southern Java has the potential to trigger an earthquake with magnitude of Mw 8.90-8.94. Meanwhile, the Bali-Sumbawa subduction segment has potential to trigger earthquake with maximum magnitude of Mw 9.08. All the results of the estimated maximum earthquake magnitude presented can be considered in seismic hazard modeling for subduction earthquake sources based on which scenario will be selected as the earthquake and tsunami simulation approach.

5. CONCLUSION

Located near the confluence of Indo-Australian and Eurasian plates, Java Island and its surroundings are prone to earthquakes. Subduction zones that are long enough with different velocities and seafloor ages show variations in the seismic properties of each segment. We observed that the dipping angle of the Java subduction zones is steeper than that of Sumatra. This phenomenon is associated with the oceanic crust age submerged beneath southern Java, which is older than Sumatra. The spatial variation in a-value and b-value have been mapped. Moreover, these a-b parameters for each subduction segment have been comprehensively presented. It is observed that there is a similar pattern of a-values and b-values. The regions with low b-values relatively fit the large earthquake locations. Based on the subduction zone modeling analysis, the low a-values and b-values are in the south coast of West Java and south coast of Central-East Java. We found that the most significant earthquakes in subduction zone were consistent with relatively high fractal dimension (D values) and low b-values. However, further research is needed to investigate these correlations more appropriately.

For the return period of 100 to 500 years, the Java interplate segments have the estimated maximum earthquake magnitude of Mw 8.47-9.00, assuming that all the tectonic energies in those areas were released seismically. Although there has been no earthquake with a magnitude greater than Mw 8.0 occurring along the Java trench, with the mechanism and seafloor age being similar to those in the east-north side of Japan, which triggered the 2011 Tohuku earthquake of Mw 9.0, these results are worth considering. Such findings can also become one of the references for future seismic hazard studies, earthquake and tsunami disaster mitigation plans in Java and its surroundings.

6. ACKNOWLEDGMENT

The authors would like to thank the Meteorological, Climatological, and Geophysical Agency (BMKG) Indonesia for providing earthquake data and information.

7. REFERENCES

[1] Roy S., Ghosh U., Hazra S., and Kayal J. R., Fractal Dimension and b-value Mapping in the Andaman-Sumatra Subduction Zone, Nat Hazards, Vol. 57, 2011, pp.27–37.

[2] Sieh K. and Natawidjaja D., Neotectonics of the Sumatran Fault, Indonesia, Journal of Geophysical Research: Solid Earth, Vol. 105, Issue B12, 2000, pp.28295-28326.

[3] Ammon C. J., Kanamori H., Lay, T. and Velasco A. A., The 17 July 2006 Java Tsunami Earthquake. Geophysical Research Letters, Vol. 33, Issue 24, 2006, pp.1-5.

[4] Tsuji Y., Imamura F., Matsutomi H., Synolakis C. E., Nanang P. T., Jumadi, Harada S., Han S. S., Arai K., and Cook B., Field Survey of the East Java Earrthquake and Tsunmai of June 3, 1994., Pure and Applied Geophysics, Vol. 144, Issue 3, 1995, pp.839-854.

[5] Abercrombie R. E., Antolik M., Felzer K., and Ekström G., The 1994 Java Tsunami Earthquake: Slip Over a Subducting Seamount, Journal of Geophysical Research, Vol. 106, Issue B4, 2001, pp.6595-6607.

[6] Okal E., The south of Java earthquake of 1921 September 11: A negative search for a large interplate thrust event at the Java Trench, Geophysical Journal International, Vol. 190, Issue 3, 2012, pp.1657-1672.

[7] Setiyono U., Gunawan I., Priyobudi, Yatimantoro T., Imananta R.T., Ramadhan M., Hidayanti, Anggraini S., Rahayu R.H., Hawati P., Yogaswara D.S., Julius A.M., Apriani M., Harvan M., Simangunsong G., and Kriswinarso T., Catalog of Significant and Destructive Earthquakes 1821-2018, Earthquake and Tsunami Center of BMKG Indonesia., (Katalog Gempabumi Signifikan dan Merusak tahun 1821-2018, Pusat Gempabumi dan Tsunami BMKG Indonesia), 2019, pp.1-278.

[8] Diaz L. P., Regional Geology and Tectonics (Second Edition), Vol. 1: Principle of Geologic Analysis, Chapter 3 – Age of the Oceans, 2020, pp.21-40.

[9] Müller R. D., Sdrolias M., Gaina C., and Roest W. R., Age, Spreading Rates and Spreading Symmetry of the World's Ocean Crust, Geochemistry, Geophysics, Geosystems, Vol. 9, Issue 4, 2008, pp.1-19.

[10] Norio O., Ye T., Kajitani Y., Shi P., and Tatano H., The 2011 Eastern Japan Great Earthquake Disaster: Overview and Comments, International Journal of Disaster Risk Science, Vol. 2, Issue 1, 2011, pp.34-42.

[11] Mimura N., Yasuhara K, and Kawagoe S., Damage from the Great East Japan Earthquake and Tsunami – A quick report, Mitigation and Adaptation Strategies for Global Change, Vol. 16, Issues 7, 2001, pp.803-818.

[12] Hartoko A., Helmi M., Sukarno M., and Hariyadi, Spatial Tsunami Wave Modelling for The South Java Coastal Area, Indonesia. International Journal of Geomate, Vol. 11, Issue 25, 2016, pp.2455-2460.

[13] Widiyantoro S., Gunawan E., Muhari A., Rawlinson N., Mori J., Hanifa N. R., Susilo S, Supendi P, Shiddiqi H. A., Nugraha A. D., and Putra H. E., Implications for Megathrust Earthquakes and Tsunamis from Seismic Gaps South of Java Indonesia. Scientific Reports, 10, 15274, 2020.

[14] Nugraha A. D., Shiddiqi H. A., Widiyantoro S., Thurber C. H., Pesicek J. D., Zhang H., Wiyono S. H., Ramdhan M., and Irsyam M., Hypocenter Relocation along the Sunda Arc in Indonesia, Using a 3D Seismic-Velocity Model, Seismological Research Letters, Vol. 89, Issue 2A, 2018, pp.603–612.

[15] International Seismological Centre, http://www.isc.ac.uk, ISC-EHB data set, International Seismological Centre, 2020, Thatcham, United Kingdom.

[16] Engdahl E. R., Di Giacomo D., Sakarya B., Gkarlaouni C. G., Harris J., and Storchak D. A., ISC- EHB1964‐2016, an Improved Data Set for Studies of Earth Structure and Global Seismicity, Earth and Space Science, Vol. 7, Issue 1, 2020, pp.1-13.

[17] Gardner J. K, and Knopoff, L., Is the Sequence of Earthquakes in Southern California, with Aftershocks Removed, Poissonian?, Bulletin of the Seismological Society of America, Vol. 64, Issue 5, 1974, pp.1363–1367.

[18] Reasenberg P., Second-order Moment of Central California Seismicity, 1969–1982, Journal of Geophysical Research: Solid Earth, Vol. 90, Issue B7, 1985, pp.5479–5495.

[19] Uhrhammer R. A., Characteristics of northern and central California seismicity, Earthquake Notes, Vol. 57, Issue 21, 1986 (abstract).

[20] Zaliapin I., and Ben-Zion Y., Earthquake Clusters in Southern California I: Identification and Stability, Journal of Geophysical Research: Solid Earth, Vol. 118, Issue 6, 2013, pp.2847–2864.

[21] Zhuang J., Ogata Y., and Vere-Jones D., Stochastic Declustering of Space-time Earthquake Occurrences, Journal of the American Statistical Association, Vol. 97, Issue 458, 2002, pp.369–380.

[22] Teng G. and Baker J. W., Seismicity Declustering and Hazard Analysis of the Oklahoma-Kansas Region, Bulletin of the Seismological Society of America, Vol. 109, Issue 6, 2019, pp.2356-2366.

[23] Ogata Y., Statistical Models for Earthquake Occurrences and Residual Analysis for Point Processes, Journal of the American Statistical Association, Vol. 83, Issue 401, 1988, pp.9–27.

[24] Ogata Y., Space-time Point-process Models for Earthquake Occurrences, Annals of the Institute of Statistical Mathematics, Vol. 50, Issue 2, 1998, pp.379–402.

[25] Susilo A., Hisyam F., and Wasis, Earthquake Analysis in East Java, Indonesia between 1960-2017 using Markov Chain Model, International Journal of Geomate, Vol. 17, Issue 63, 2019, pp.149-156.

[26] Gutenberg B. and Richter C., Frequency of earthquakes in California. Bulletin of the Seismological Society of America, Vol. 34, Issue 4, 1944, pp.185–188.

[27] Utsu T., A method for Determining the Value of b in a Formula log n = a - bM Showing the Magnitude-Frequency Relation for Earthquakes. Geophys. Bull. Hokkaido Univ., Vol. 13, 1965, pp.99–103.

[28] Rohadi S., Grandis H., and Ratag M. A., Studi Variasi Spasial Seismisitas Zona Subduksi Jawa (Study of the Spatial Variation for Java Subduction Zone Seismicity), Jurnal Meteorologi dan Geofisika, Vol. 8, Issue 1, 2007, pp.42-47.

[29] Grassberger P. and Procaccia I., Characterization of Strange Attractors, Physical Review Letters, Vol. 50, Issue 5, 1983, pp.346-349.

[30] Kumar A., Rai S. S., Joshi A., Mittal H.,

Sachdeva R., Kumar R., and Ghangas, V., The b-value and Fractal Dimension of Local Seismicity around Koyna Dam (India), Earthquake Science, Vol. 26, Issue 2, 2013, pp.99-105.

[31] Hanks T. C. and Kanamori H., A Moment Magnitude Scale, Journal of Geophysical Research, Vol. 84, Issue B5, 1979, pp.2348–2350.

[32] Wells D. L. and Coppersmith K. J., New Empirical Relationships among Magnitude, Rupture Length, Rupture Width, Rupture Area, and Surface Displacement, Bulletin of the Seismological Society of America, Vol. 84, Issue 4, 1994, pp.974-1002.

[33] Wiemer S., A Software Package to Analyze Seismicity: ZMAP, Seismological Research Letters, Vol 72, Issue 3, 2001, pp.373-382.

[34] Berggren W. A., Kent D. V., Flynn J. J., and Van Couvering J. A., Cenozoic Geochronology, Geological Society of America Bulletin., Vol. 96, Issue 11, 1985, pp.1407-1418

[35] Muntafi Y., Widodo, and Makrup L., Analisis Hazard Gempa DKI Jakarta Metode Probabilistik dengan Pemodelan Sumber Gempa 3 Dimensi (Seismic Hazard Analysis of Jakarta Special Region using Probabilistic Method with 3-Dimensional Earthquake Sources Modeling), Teknisia, Vol. XX, Issue 2, 2015, pp.85-95.

[36] Ashadi A. L., Harmoko U., Yuliyanto G., and Kaka S. I., Bulletin of the Seismological Society of America, Vol. 105, Issue 3, 2015, pp.1711–1720.

[37] Nugraha A. D., Shiddiqi H.A., Widiyantoro S., Sutiyono., and Handayani T., Analysis of Spatiotemporal Variation in b-value for the Sunda Arc using High Precision Earthquake Location, AIP Conference Proceedings, Vol. 1730, Issue 1, 2016, pp.1-6.

[38] Suananda Y. I. B., Aufa I., and Harlianti U. Identifying Intraplate Mechanism by b-value calculations in the South of Java Island, IOP Conferences Series: Earth and Environmental Science, Vol. 132, 012032, 2018, pp.1-7.

[39] Stein S. and Wysession M., An Introduction to Seismology, Earthquakes, and Earth Structure, Geological Magazine, Vol. 140, Issue 6, 2003, pp. 733-734.

[40] Hanifa N. R., Sagiya T., Kimata F., Efendi J., Abidin H. Z., and Meilano I., Interplate Coupling Model off The Southwestern Coast of Java, Indonesia, based on Continuous GPS data in 2008-2010. Earth and Planetary Science Letters, Vol. 401, 2014, pp.159-171.

[41] Nugroho H. A., Joelianto E., and Puspito N. T., Characteristic of Earthquake Occurrences based on Chaotic Analysis and Fractal Dimension, Conference proceedings, IEEE Conference on Control, Systems and Industrial Informatics, 2012, pp. 208-213.

[42] National Center for Earthquake Studies (PuSGeN). Indonesian Seismic Sources and Seismic Hazard Maps 2017. Center for Research and Development of Housing and Resettlement, Ministry of Public Works and Human Settlements, (Peta Sumber dan Bahaya Gempa Indonesia Tahun 2017. Pusat Litbang Perumahan dan Pemukiman, Kementerian Pekerjaan Umum dan Perumahan Rakyat), 2017, pp 1–377.